

FLOATING OFFSHORE WIND TURBINE ROTOR OPERATING STATE - MODIFIED TIP LOSS FACTOR IN BEM AND COMPARISON WITH CFD

Krishnamoorthi Sivalingam¹, Srikanth Narasimalu²

Wind and Marine Renewables, Energy Research Institute @ NTU
Nanyang Technological University

1 Cleantech Loop, #05-08, Cleantech One, Singapore 637141

skrishnamoorthi@ntu.edu.sg

nsrikanth@ntu.edu.sg

Abstract— Abundant and consistent wind resource of deep water ocean have attracted offshore wind energy industry to look for the possible expansions and adoption of various oil and gas floating platform technologies. This has compelled the industry to venture in to floating offshore installations for wind turbines. The floating installations lead to complex rotor motions in 6 degrees of freedom.

The current study focuses on the dynamic effects of the platform pitching motion on the rotor aerodynamics for OC3 phase IV case 5.1 with modified wave height. High fidelity CFD (Computational Fluid Dynamics) software was employed along with semi empirical tool, FAST developed by NREL, USA by assuming the wind turbine as a rigid body.

The hydrodynamic effects leading to the pitching motion of the turbine platform are obtained from FAST. These pitching motions are coupled with the rotating blades to study transient flow behaviors using CFD. The results are compared with the standard BEM based methods having modified Prandtl tip loss factor. The results show that the increased wave height induces very high velocity and acceleration of the platform motion and thereby on the rotor plane. Moreover this confirms that the turbine is operating both in windmill and turbulent state under such conditions. BEM validity with Glauert correction and validity of tip loss model is to be further assessed for the application of floating offshore wind turbine performance and design predictions.

Index Terms— BEM, Induction factor, OC3 phase IV, FAST, Simulation, NREL 5MW, AeroDyn, turbulent state, CFD, Floating offshore wind turbine.

I. NOMENCLATURE

B	- number of blades
BEM	- blade element momentum
C_l	- co-efficient of lift
C_d	- co-efficient of drag
C_T	- co-efficient of thrust
dr	- blade element length in radial direction
dT	- elemental torque (BEM based)

dF	- elemental thrust (BEM based)
dTCFD	- CFD based elemental torque
dFCFD	- CFD based elemental thrust
F	- overall loss factor
Ft	- prandtl tip loss factor
Fh	- hub loss factor
FAST	- Fatigue, Aerodynamics, Structures, and Turbulence code
FOWT	- floating offshore wind turbine
MRF	- multiple reference frame
OC3	- Offshore Code Comparison Collaboration
r	- blade element distance from the centre of the rotor
TSR	- tip speed ratio
U	- local wind speed
U_∞	- free stream wind speed
ρ	- air density
Ω	- rotational speed of the rotor
ω	- rotational speed of wake
φ	- local flow angle
σ'	- local solidity

II. INTRODUCTION

The commitment to achieve the target in reducing carbon emissions by most countries draws greater interest towards

carbon free energy sources. Renewable energy sources are expected to occupy a major share in total energy supply as predicted by UK [1] and EU [2]. Of all renewable energy sources such as solar, tidal and wave, wind is more economically viable as indicated in [3]. Most onshore ideal locations are exploited to the fullest and hence the wind industry focuses on offshore locations where windspeed is higher and steadier. Installation costs of offshore wind turbines are proportional to the water depth for the conventional turbines with bottom support structures such as monopile towers and are limited by water depth. Floating wind turbines are independent of water depth and hence more studies are focused towards the development of such floating designs and associated structures [4]. Several prototypes have been tested in the past decades, which are helpful in migrating from shallow waters to deeper waters. For example Hywind, a spar design floating wind turbine was deployed in Norwegian waters [5] and Windfloat, a semi-submersible floating wind turbine deployed off Portugal [6].

The floating wind turbines should be economical in both capital and operating cost. Their cost per kWh of wind generated power should be comparable to conventional energy sources for a sustainable market. Apart from installation cost, the turbine has to survive the harsh environments in deep water. The cost can be substantially reduced by developing a numerical model that accounts for all the complex interactions. Currently only prototypes have been deployed and hence costs are bound to be higher than more mature technologies. In order to reduce costs it will be necessary that the designs of floating wind turbines are not overly conservative. This will require a numerical model of the design to be created with sufficient detail to allow all aspects of the system to be considered.

Floating offshore wind turbine (FOWT) is a complicated system as it has several components with complex interactions. Total loading of the FOWT is a resultant of all interactions. In order to make more accurate numerical models all aspects of the wind turbine must be included in the same model.

Numerical performance prediction of FOWT is critical and challenging to accurately assess the aerodynamic loads. Most of the commercial and open source wind turbine software employs BEM methods to determine the loads. The BEM method is well proven as it has been outlined in several publications [7] and successfully applied for bottom fixed wind turbine during its design cycle [8]. As it has been discussed [8], the BEM method can be extended for FOWT as long as the assumptions are valid for a range of wave and wind conditions to predict FOWT rotor performance.

The effect of rotor plane pitching motion on the aerodynamic performance of FOWT [9] due to the regular 6m wave height and a CFD based induction factor development methodology [10] are developed for the OC3 phase IV case 5.1 [11]. It was shown that [9] that 6-m, 10-s sea state lets the turbine to operate in the windmill state until the axial induction factor of complete rotor was not exceeding 0.4. In the current study the thrust loading of the rotor is increased purposely by varying the rotor plane velocity to force the turbine to operate in turbulent state or beyond. The forced transition from windmill state to turbulent state is to validate the accuracy of BEM by comparing with fine details of the flow from CFD results. The transition can be achieved by increasing the wave

height from 6-m to 12-m and maintaining the 10-s wave period

for the OC3 phase IV case 5.1 as shown in Fig. 1. Increase in the wave height will intensify the pitch rate of the spar buoy floating platform leading to an increased angular velocity and acceleration of the rotor plane. This continuously changes the relative wind speed of rotor and thereby affecting the various resultant forces. When the turbine is working in different wind turbine operating conditions for a particular pitching motion, it is important to quantify the error associated in predicting the FOWT performance by BEM method which is basically derived for bottom fixed turbine. As the BEM is mostly used in wind turbine design certification process where normally more than 6000 simulation cases (CFD and FEA tools can not be employed for all simulations) are to be performed, the purpose of this research scope is considered as an important. Moreover, the prediction of fine variation of rotor power/load due to dynamic pitching of the floating platform is also equally important for an accurate fatigue life assessment. This leads to the usage of high fidelity CFD tool. As the study is focused on the applied forces on the rotor to check the validity of BEM model for an academic research purpose in FOWT applications, no blade control strategy is considered.

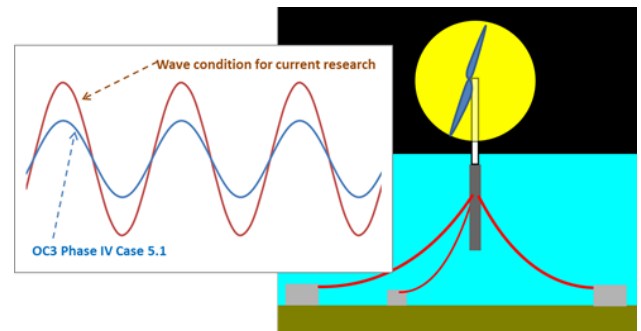


Fig. 1 Comparison between OC3-Phase IV case 1 wave condition and the regular wave condition adopted for this research work

III. METHODOLOGY AND APPROACH

The wind loadings and its impacts are fundamental design parameters for the overall design of FOWT structures and its components. An accurate prediction of aerodynamic forces is inevitable for the design of reliable and efficient wind turbine. Various mathematical models such as BEM methods, prescribed or free wake vortex methods, acceleration potential methods and CFD techniques are commonly employed to predict the aerodynamic loads for onshore turbines. Those methods are originally evolved from helicopter aerodynamics and are being applied in wind turbine design. BEM method is widely used for wind turbine rotor design and can be integrated as a module in various servo-elastic-aero tools for system level performance predictions due to its high computational efficiency. Since BEM code's are highly flexible to include various corrective models, such as wake expansion correction, blade root and tip losses corrections, it can be tweaked with the appropriate corrective models that are specific FOWT application.

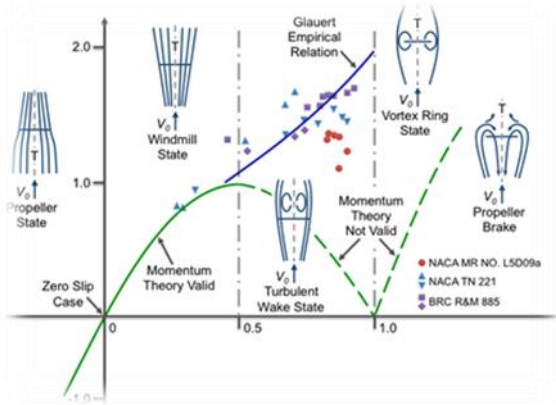


Fig. 2. Axial induction factor Vs Thrust/thrust co efficient (Eggleston and Stoddard,1987).

Previous studies shows that pitching motion of the spar buoy floating platform for OC3 phase IV case 5.1 conditions does not influence the wind turbine operating state with specified wave characteristics [9]. The induction factor has a direct correlation with the wind turbine operating state. The preferred windmill state will be retained as long as the induction factor does not exceed 0.5 even with the platform pitching motion. The relation between axial induction factor and coefficient of thrust with the corresponding wind turbine operating state based on the momentum theory is shown in Fig. 2. Some sector of the wind turbine rotor is expected to operate in the turbulent wake state, when the axial induction factor tips over 0.5, due to increase in wave height to 12m. The accuracy of the traditional BEM can be validated when the FOWT is operating in the turbulent wake state, though this is impractical in real world scenario .

The default operating state of a wind turbine is windmill state when there is a steady flow field. Since FOWT is not constrained in any of 6 degrees of freedom, the continuous pitching motion at the rotor plane will result in the transient flow field causing the wind turbine to oscillate between windmill and propeller state. Wave induced floating platform pitching motion causes a rapid drop in effective wind speed at the rotor plane resulting in higher tip speed ratios. The BEM theory is not able to model the constant transitions between the operating states of the wind turbine accurately. The problem is further compounded by the platform surge and high pitch rate. Thus, the application of BEM method for modelling unsteady aerodynamics for FOWT is uncertain.

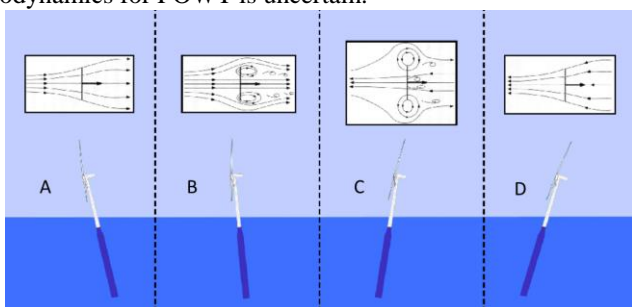


Fig. 3. Extreme platform pitching motion and the resulting flow filed

The hypothetical FOWT [12] shown in Fig. 3 (from A to D) illustrates how this transition occurs between different states

of the wind turbine during platform pitching motion and the wind speed. Initially, the turbine will operate in the windmill state (A) when the platform pitching motion is minimal, extracting energy from the flowfield. Wind turbine rotor may interact with its own wake during rotor plane pitching along the flow direction, which may result in the formation of a turbulent region (B), predominanaty near tip regions. At some point, illustrated in the region (C), a toroidal recirculation flow path normal to the rotor disk may develop named as vortex ring state (VRS). In the VRS state, thrust and torque are driven by the rate of energy dissipation in to the vortex ring and the momentum balance equations may break down as with scenario B (moreover, when axial induction factor exceeds 0.4) and the pitching motion may impart energy into the flowfield and behave like a propeller. In addition to the periodic changes in aerodynamic loads during pitching motion, it may also violate the momentum slip-stream assumption [13]. The accuracy of wind turbine design tools such as FAST are questionable which uses AeroDyn which in turn based on momentum balance equation for their BEM based calculations [14]. All industrial codes for wind turbine design are developed and only applicable for fixed bottom wind turbine for static rotor plane.

The induction factors are incorporated in the BEM equations to deduce the aerodynamic loads on the rotor. By accurately predicting the aerodynamic load, the induction factor can be obtained from the BEM equations. CFD simulations can determine the aerodynamic loads more precise than BEM theory for the prescribed conditions. As the axial induction factor is expected to go beyond 0.4, CFD based induction factor derivation methodology as stated in [9][10] can not be applied as such. Axial induction factors above 0.4 have to be corrected for Glauert correction and accurate tip loss model. Outcome of this study is to compare power and thrust values obtained from traditional BEM theory axial induction factor and the CFD based axial induction factor in the turbulent wake state.

The CFD simulation was set-up based on chosen case scenario from an existing analytical tool called FAST for one to one comparison. FAST is a modularised software developed by NREL for the design calculations including hydrodynamics, aerodynamics, structural mechanics, control systems etc.[15] for on and offshore wind turbine applications. The CFD simulations were carried out with known steady state case at the uniform wind speed of 8m/s with available ANSYS CFD code (Version 15) and the rotor power was compared with the value given by design curve to gain the confidence on the results as in [9] and [10]. The simulation setup includes the mesh parameters and boundary condition initialization as per [9] and [10], the calculations were carried out for the chosen turbine motion scenario of 12-m wave height and 10-s wave period.

FAST solver was modified in this study to extend its applicability to floating offshore wind turbines. FAST computes the aerodynamic loads on the wind turbines through AeroDyn, a separate module embedded in FAST. AeroDyn is an aeroelastic simulation module to predict the wake behaviour of horizontal axis wind turbines based on BEM theory and the generalized dynamic-wake theory [16]. BEM theory is

extensively used by wind turbine designers and generalized dynamic wake (GDW) theory is a recent addition to model the skewed and unsteady wake dynamics, which traditional BEM theory lacks. BEM theory is opt for this study, as it is flexible in accommodating various new models such as hub and tip loss models and Glauert correction term. The two tip loss models (Prandtl and Georgia Tech) embedded in the AeroDyn is not so accurate compared to CFD results [9] for the chosen scenario.

As in OC3, 5MW NREL wind turbine was chosen for this study as required data for comparison are readily available [17]. To compare and bench mark the results, OC3 Phase IV cases (with minor modifications and increased wave height) were considered [11][18]. A 3D blade model was created with chord and twist details obtained from NREL 5MW wind turbine using lofting option, as said before, the rotor is a rigid body rotating in a fixed rotor plane. The input for the pitching motion characteristics is achieved through CCL, a command prompt for CFX tool. The simplified approach enable us to focus on the aerodynamics of the blades, as the objective of the current work is to characterize the induced velocities of FOWT rotor and to compare against BEM results to quantify the accuracy. This will enhance the quality of FAST tool in the rotor design process as CFD tools are laborious and computationally intensive. But CFD helps to visualize and understand the basic flow phenomena, which FAST is not capable of (such as turbulence region development, vortex ring state and propeller state as in Fig. 3).

A. Axial and Tangential Induction Factors in BEM

As discussed in detail [10], the axial and the tangential induction factors are two vital most important factors that a BEM code operates iteratively. Axial induction factor can be defined as the fractional decrease in wind velocity between the free stream and the FOWT rotor. It is important to emphasize here that the wake rotation is only important for high torque (or low TSR) and tangential induction is not usually very important for modern utility-scale turbine rotors. Flow through the rotor in the axial direction is determined by the axial induction factor, a , and the rotation of the wake behind the turbine is determined by the tangential induction factor, a' , expressed as

$$a = 1 - \frac{U}{U_\infty} \quad (1)$$

$$a' = \frac{\omega}{2\Omega} \quad (2)$$

The aerodynamic forces are calculated based on these parameters along with the empirical coefficients for each blade sections including the additional loss/correction factors. The tip (F_{new}) and the hub losses (F_h) are accounted for losses at tip and hub. Current study includes modified Prandtl tip loss function of Georgia Institute of Technology to account for the tip losses. The total loss factor is calculated as

$$F = F_{new} \times F_h \quad (3)$$

Prandtl tip loss factor:

$$F_t = \left(\frac{2}{\pi}\right) \cos^{-1} e^{-f}$$

Modified Prandtl tip loss factor based on the Navier-Stokes solutions of Xu and Sankar (2002), Georgia Institute of Technology:

$$F_{new} = \begin{cases} -\frac{F_t^{0.85} + 0.5}{2} & \text{for } 0.7 \leq r/R \leq 1 \\ \left(1 - \left(\frac{r}{R}\right) \left(1 - F_{r=\frac{0.7}{R}}\right)\right) / 0.7 & \text{for } r/R < 0.7 \end{cases}$$

When $CT \leq 0.96F$, the standard BEM theory is used to calculate the axial induction:

$$a = \left[1 + \frac{4F \sin^2 \phi}{\sigma r (C_{1t} \cos \phi + C_{2t} \sin \phi)}\right]^{-1} \quad (4)$$

If $CT > 0.96F$, the element is highly loaded and the modified Glauert correction will be used to determine the new axial induction factor:

$$a = \left(18F - 20 - 3\sqrt{C_T(50 - 36F) + 12F(3F - 4)}\right) / (36F - 50) \quad (5)$$

Accurate flow physics can be captured by incorporating additional loss functions such as skewed wake correction etc. The axial induction factor will be updated with Glauert correction, when the wake induced pitching motion tends to increase the value beyond 0.4.

A. Elemental Torque and Thrust

The BEM code solves a set of equations iteratively [10] to calculate the induction factors and thereby the forces on the blade elements. Torque and thrust on the blade elements are given by the equations (6) and (7) respectively,

$$dT = 4\pi r^2 dr \rho U_\infty F (1 - a) a' \Omega \quad (6)$$

$$dF = 4\pi r dr \rho U_\infty^2 F (1 - a) a \quad (7)$$

dT is the elemental torque, dF is the elemental thrust, F is the combination of hub loss and Georgia Tech modified Prandtl tip loss factors, a is the axial induction factor and a' is the tangential induction factor. The present work is focussed on comparing the thrust and rotor power values between BEM and CFD results. CFD based induction factor derivation methodology will be developed for turbulent state by extracting the Glauert correction factor and accurate tip loss model terms from BEM based equations to compute CFD based induction factor. Upon obtaining the validated CFD based induction factor derivation methodology, the CFD based results will be compared against BEM prediction to quantify the accuracy level for FOWT applications and control algorithm development as mentined earlier.

IV. FAST SIMULATION SCENARIO FOR CFD MODEL SETUP AND COMPARISON

The basis for the current study is OC3 Phase IV FAST model. The model was refined to cover the requirements of current simulations as listed below in the FAST model settings. This model includes mooring line and aerodynamic models to simulate time series of the turbine and platform responses to environmental and operating conditions.

In Phase IV of OC3, case 5.1 injects regular sea wave motions (modified with 12m wave height instead of 6m) and steady wind excitation. The tower is initialized at its static position, and wind and waves are introduced with parameters shown in Table 1.

Table 1.
FAST simulation scenario:

Uniform wind speed (m/s)	Sea State	Rigid body assumption	Rotor speed rpm
8	12m wave height and 10 sec wave period	Yes	9.16

FAST model settings are as follows:

- The tower fore-aft and side-side DoFs were switched off to make rigid body.
- First and second flapwise blade DoF were switched off and edgewise DoF was also switched off to make rigid body.
- An equilibrium BEM inflow model was used along with Georgia Institute of Technology's corrected Prandtl tip loss function (GTECH).
- Blade pitch and generator torque controllers were switched off.
- Free-stream wind was defined as constant, unidirectional, and without shear.
- The six platform DoFs were enabled.

Wind and wave data from OC3 Phase IV case 5.1 were used to define the sea state in terms of wave height, H, and wave period, T. The simulated time series was created with these parameters. Time domain simulations were performed as per the case described in Table 1, with each simulation lasting 1860seconds. The outputs generated by the initial 1800 seconds of each simulation were omitted in the analysis as to make sure all the transient start up effects to be removed.

The initial run was performed to extract the motion of the platform for the above specified OC3 case. The Fig. 4 represents the roll, pitch and yaw motions of the platform for the wave conditions specified in Fig. 5.

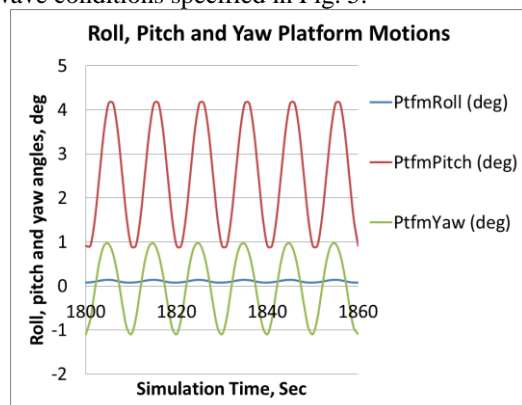
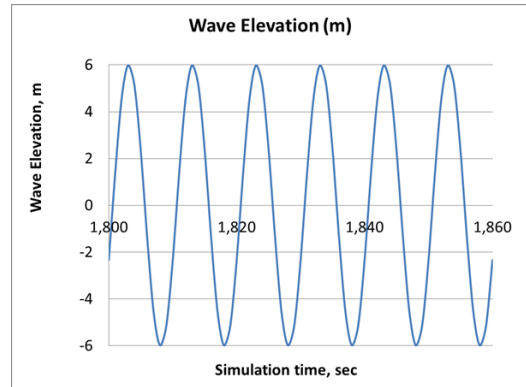


Fig. 4. Platform motions for the simulation scenario as in Table 1



V. FIG. 5. WAVE ELEVATION PROFILE FOR TABLE 1 CASE

As seen in Fig. 4, pitching motion is only considered for the study as it is dominant when compared to yaw and roll and hence the later is omitted. For the chosen scenario the mean rotor tilt was found to be 2.54 degrees. As the study focuses on platform pitching motions on the rotor plane aerodynamics, the platform rotations were transformed in to the rotor plane motions at the hub height.

V. CFD BASED NUMERICAL ASSESMENT

The CFD simulations were set-up for FAST OC3 phase IV 5.1 case for NREL 5MW, modified to incorporate 12m significant wave height which was used for hydrodynamics calculations. The resulting turbine motions provided by FAST were included in the CFD simulations. Steady state and mean position simulation were run as per the Table 1 data. Steady state power prediction by BEM and CFD were 1.659 MW and 1.76 MW respectively. The steady state CFD results are the initialization values for transient CFD simulation.

A. MRF and Sliding Mesh Simulation Methodology

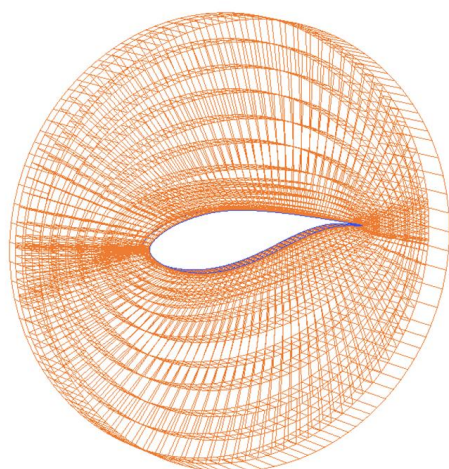
The pitching motion and its dynamic effects on the rotor plane are well understood by CFD simulations of the NREL 5MW turbine. The steady state (Multiple Reference Frame) MRF simulations were carried out by tilting the rotor to mean pitch angle of 7.54 degrees (2.54 mean pitching angles along with a 5 degrees main shaft tilt). The mean rotational speed and the wind speeds used in CFD simulations are as shown in Table 1. The results of the steady state calculations were used to initialise the transient case involving the pitching motion of the turbine. The pitching motion methodology was developed in ANSYS-CFX (Version 15). The domains are structured in such a way that both the blade rotations and rotor pitching motions could be handled smoothly by the solver. The rotor domain had a sliding mesh interface for blade rotations and the mesh motion applied for pitching had an extremely high stiffness in this domain which was relaxed gradually towards the outer domain to preserve the fine boundary layer mesh. This high stiffness ensured that the mesh in the rotor domain had almost no relative nodal displacement, as the mesh on the blade had the first node on the order of microns to yield a $y^+ \sim 3$, where y^+ is a non-dimensional wall distance for wall bounded flow.

B. Hexa Meshing Strategy

The blade geometry was generated in ANSYS ICEM CFD (Version 15) by sweeping various cross section of the NREL 5MW airfoil. The rotor was modelled without hub and the blades are extended to meet the centre of the rotor. The inlet boundary was located at ~3 rotor diameters in front of the rotor and the domain terminates at ~6 rotor diameters behind the rotor. A multiblock meshing strategy was used to create hexahedral mesh in the whole domain. ‘O-grid’ type mesh was created in the blade domains. The geometry and mesh are shown in Fig. 6 and Fig. 7 respectively. The blade was meshed to yield a y^+ of ~3 near the tip and less than 3 everywhere else.



VI. FIG. 6. NREL 5MW ROTOR WITH THE BLADE ROOTS EXTENDED AT THE HUB CENTER



VII. FIG. 7. STRUCTURED O-GRID MESH IN THE BLADE CROSS SECTION

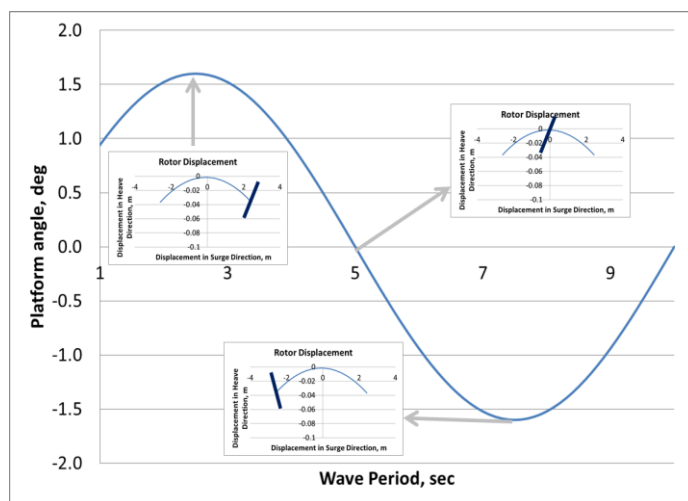
C. Rotor Plane Pitching Motion Simulation Scheme

The CFD calculations were performed for steady and uniform wind. Atmospheric boundary layer conditions were not used. The K-Omega SST was chosen as the solver. The air is considered to be incompressible air at 15°C. A high order advection scheme and first order numerical method was used for turbulence solutions. In order to understand the dynamic flow behaviour around the rotor and near wake field due to the platform pitching motion, the transient pitching motion study

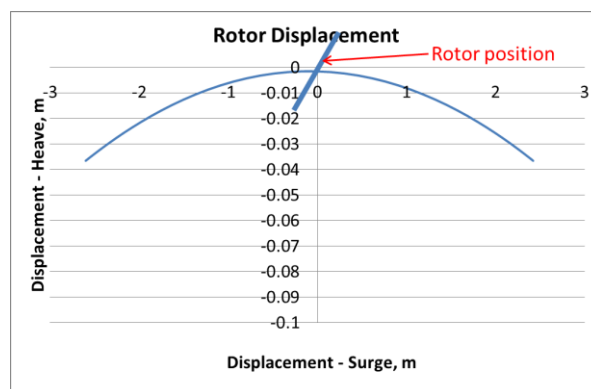
was carried out at 8m/s uniform wind speed. In this study, the transient simulation was initialised with steady state results and simulated for 70 seconds, which is 7 wave periods.

D. Coupled Dynamic Mesh Motion

The transient simulations were carried out at a single wind speed at 8m/s. The rotor pitching motion starts with the mean rotor tilt of 7.54 degrees. As the platform and tower are not modelled in this study, the pure angular motion at the platform is converted in to the translational and axis tilting motion at the rotor. The Fig. 8 & 9 shows the angular motion cycle at the platform (provided by FAST) and the corresponding rotor motion. It can be seen that, for the chosen pitching motion case, the vertical displacement is negligible and hence the horizontal displacement alone is considered in the current study. The horizontal amplitude is found to be 2.6m.



VIII. FIG. 8. PLATFORM PITCHING MOTION: ANGULAR DISPLACEMENT FOR 12M WAVE HEIGHT CONDITION WITH ROTOR POSITION



IX. FIG. 9. TRANSLATIONAL DISPLACEMENTS AT THE ROTOR FOR 12M WAVE HEIGHT CONDITION

The wind speed in the vicinity of the rotor fluctuates due to the pitching motion of the platform. In order to calculate the induction factors, the wind speed at any point on a pitching rotor is obtained using the equations below,

$$\theta = A \cdot \omega \cdot t \cdot \cos(\omega t) \quad (8)$$

$$V_{tang} = r \cdot \frac{\theta}{t} \cdot \cos(\theta)$$

$$V_{hub} = \frac{\theta}{t} \cdot 90 (\text{tower height})$$

$$V_x = V_{hub} \cdot \cos(A \sin(\omega t))$$

$$\text{wind speed} = V_x + V_{tang} + 8 \cdot \cos\left(7.54 \cdot \frac{\pi}{180}\right) \quad (9)$$

Where, ‘A’ is angular displacement amplitude at the platform, ‘r’ is the radial distance to the blade element from the hub, ‘Vhub’ is the velocity at the hub height, ‘Vx’ is the horizontal velocity of the rotor, ‘Vtang’ is the tangential velocity due to rotor pitching motion.

VI. RESULTS AND DISCUSSION

The blade was divided in to 17 segments as per FAST software with the torque and the thrust values corresponding to each segment. First three sections/elements are in the root of the blade with circular cross sections and hence will not contribute to the power production. Hence each element from 4 to 17 are compared with the corresponding elemnts in BEM model.

The flow pattern on the blades for steady state simulation was compared with previous study [19][20] to make sure that boundary layer was resolved. The flow separation region near the blade root is shown in streamline and the vector plots in Fig. 10 and 11 respectively. Also, the y+ contour plot, in Fig. 12, shows that the y+ values of the most of sections of the blade are less than 2 and close to 3 near tips.

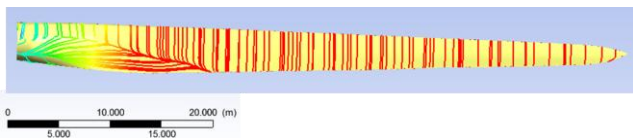


Fig. 10. Streamline plot showing the flow separation near the blade root (at $U_{\infty} = 8\text{m/s}$)

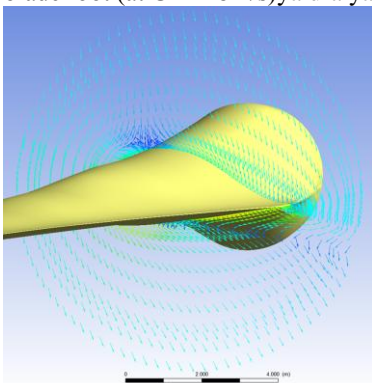
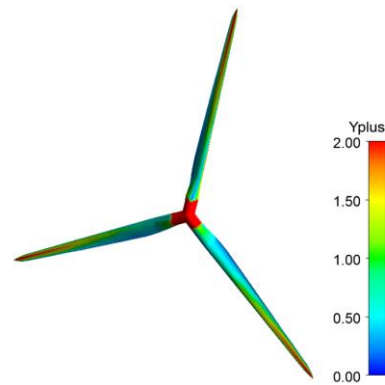


Fig. 11. Vector plot showing the flow separation at a radial distance of 8m from the root (at $U_{\infty} = 8\text{m/s}$)



X. FIG. 12. CONTOUR DISPLAYING THE Y+ VALUES ALONG THE BLADE

A. Transient Pitching Motion Results

The transient pitching motion study provides an insight about transient wake effects on every time step for one pitching cycle. Elemental thrust, power and induction factors are obtained for a set of elements (8) at 8m/s wind speed with 12m wave height for 10 equally spaced time steps in one cycle (from 41-50 sec of 70sec simulation) in Figs 14 to 21. Results are obtained for both CFD results and BEM theory to compare on the same substrate.

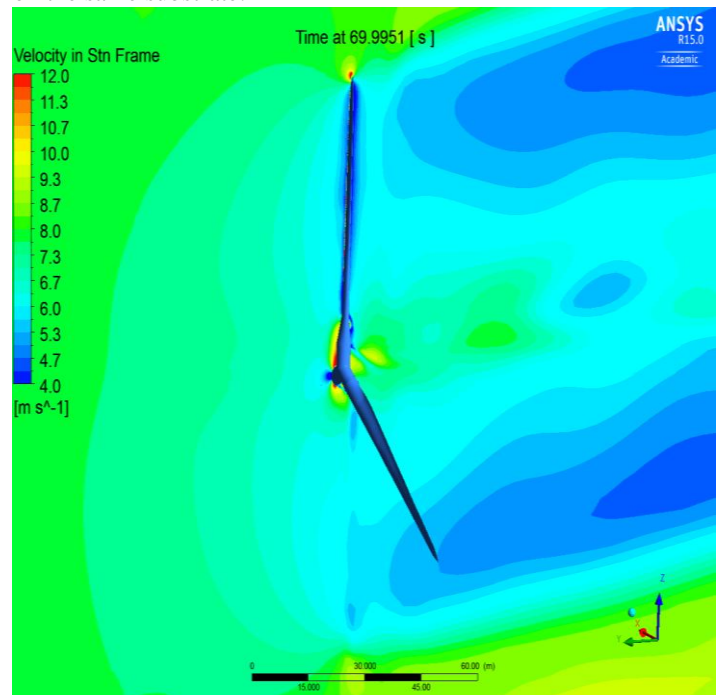


Fig. 13. Wake pattern at 70th Sec during transient pitching motion - CFD (at $U_{\infty} = 8\text{m/s}$)

The comparison of elemental power and thrust values obtained with CFD simulations and BEM based equations are given in Fig 14 to 21 selectively for 8 different elements. In the below figures, BEM (GT) refers to BEM model with modified prandtl tip loss model of Georgia Institute of Technology.

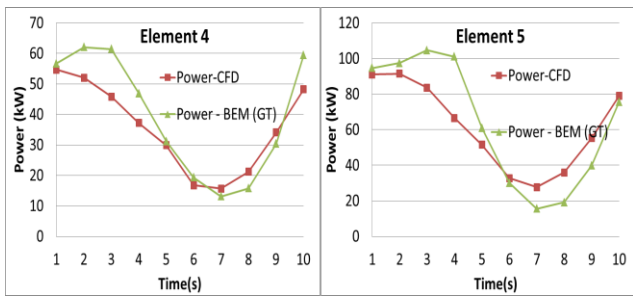


Fig. 14. Comparison of elemental power over a complete pitching motion cycle at $U_{\infty} = 8\text{m/s}$ (Element 4 & 5)

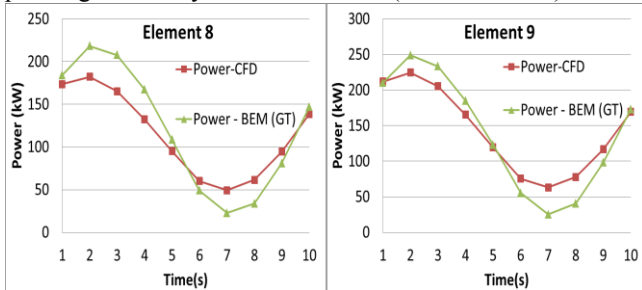


Fig. 15. Comparison of elemental power over a complete pitching motion cycle at $U_{\infty} = 8\text{m/s}$ (Element 8 & 9)

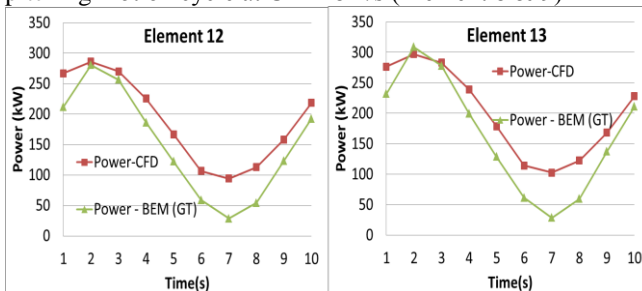


Fig. 16. Comparison of elemental power over a complete pitching motion cycle at $U_{\infty} = 10\text{m/s}$ (Element 12 & 13)

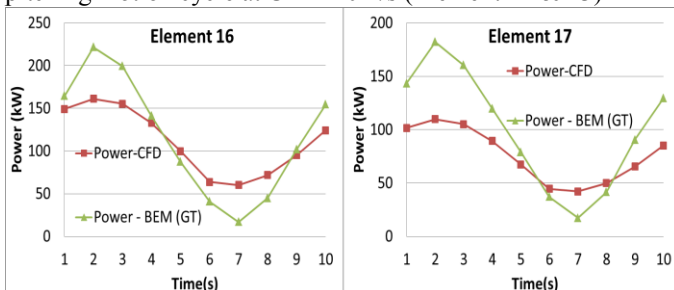


Fig. 17. Comparison of elemental power over a complete pitching motion cycle at $U_{\infty} = 10\text{m/s}$ (Element 16 & 17)

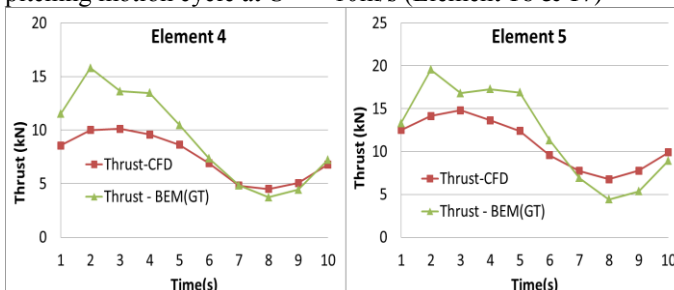


Fig. 18. Comparison of elemental thrust over a complete pitching motion cycle at $U_{\infty} = 8\text{m/s}$ (Element 4 & 5)

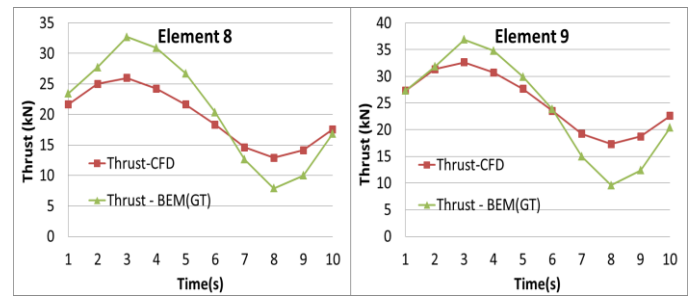


Fig. 19. Comparison of elemental thrust over a complete pitching motion cycle at $U_{\infty} = 8\text{m/s}$ (Element 8 & 9)

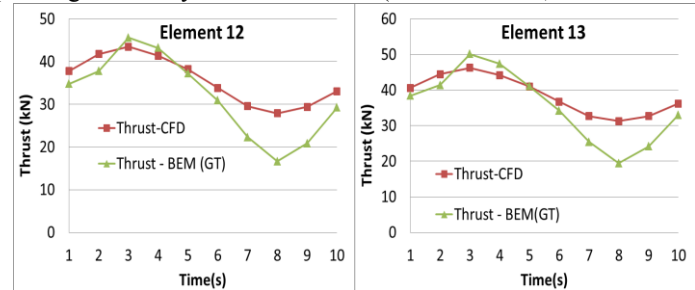


Fig. 20. Comparison of elemental thrust over a complete pitching motion cycle at $U_{\infty} = 8\text{m/s}$ (Element 12 & 13)

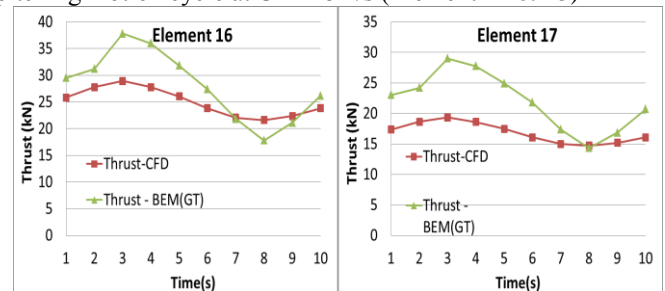


Fig. 21. Comparison of elemental thrust over a complete pitching motion cycle at $U_{\infty} = 8\text{m/s}$ (Element 16 & 17)

It is observed from the above plots that the elemental power values calculated with the BEM equations and CFD results agree qualitatively well with each other for most sections of the blade except near the tip. Though the trend is similar the values are different at large. The variation in the power prediction is higher close to the tip and this is mainly due to the effect of tip loss models used in BEM as reported in [9]. CFD predicted values are accurate than BEM for high rate of platform pitching motions. As seen in the Fig. 2 and 3, validity of BEM method is questionable when the axial induction factor exceeds 0.5 and beyond though though the model is with Glauert correction. Hence, BEM based axial and tangential induction factors are obtained from FAST simulations are compared between elements for one wave period and it is shown in the Fig. 22-24.

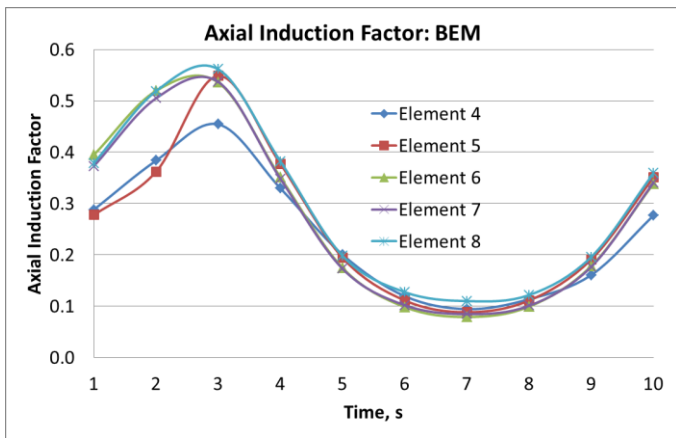


Fig. 22. Comparison of axial induction factor for the elements from 4-8 over a complete pitching motion cycle at $U_{\infty} = 8\text{m/s}$

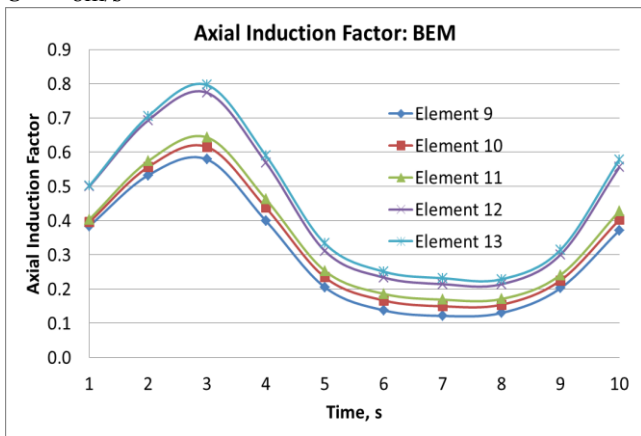


Fig. 23. Comparison of axial induction factor for the elements from 9-13 over a complete pitching motion cycle at $U_{\infty} = 8\text{m/s}$

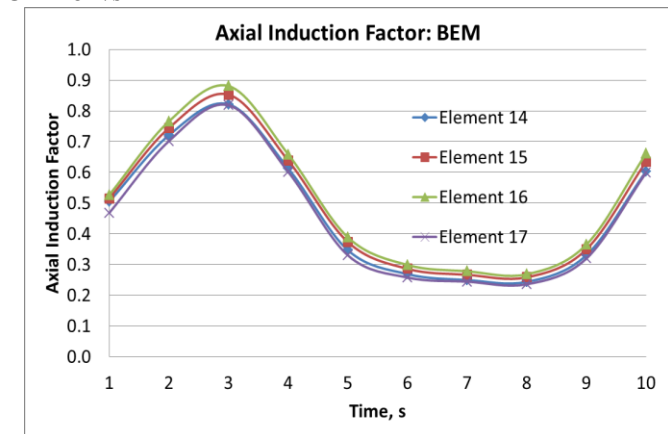


Fig. 24. Comparison of axial induction factor for the elements from 14-17 over a complete pitching motion cycle at $U_{\infty} = 8\text{m/s}$

From the plot shown in Fig. 22-24, it can be concluded that 50% of the rotor sections are at 0.5 induction factor or beyond for 25% of a wave period (approximately). This confirms the assumption that FOWT is operating in the ‘turbulent wake’ state. This leads to an action to further assess BEM equations and Glauert correction terms for FOWT applications as these are based on analytical approach and it is built upon with some basic assumptions. The tangential induction factors were also

obtained as shown in Fig. 25-27. From the axial and tangential induction factors plot one can observe a significant variation between each element and also a non uniform pattern in relation to the wave period. The substantial variations are due to blade-wake interactions during the platform pitching. In order to make sure the validity of BEM, all the empirical equations are to be further studied and compared against with CFD and experimental simulations.

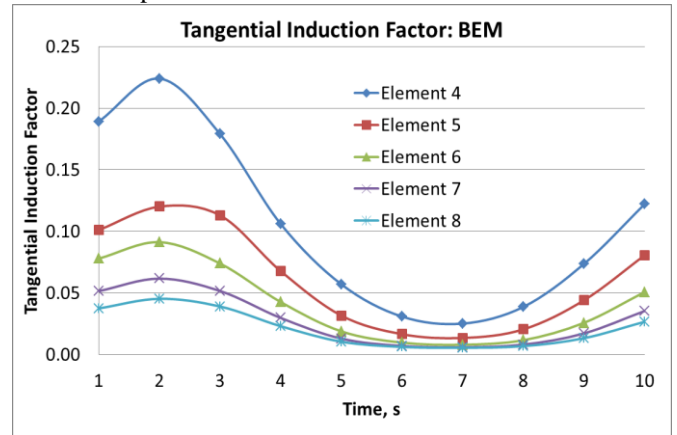


Fig. 25. Comparison of tangential induction factor for the element 4-8 over a complete pitching motion cycle at $U_{\infty} = 8\text{m/s}$

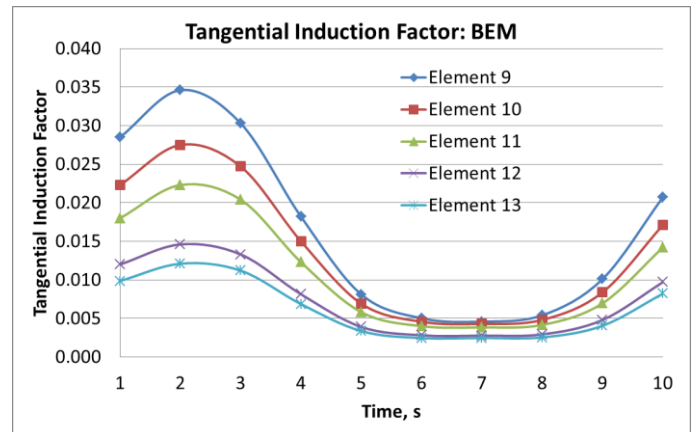


Fig. 26. Comparison of tangential induction factor for the elements 9-13 over a complete pitching motion cycle at $U_{\infty} = 8\text{m/s}$

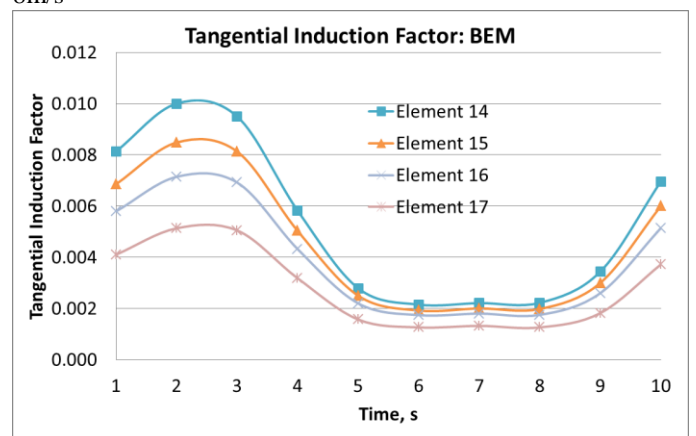
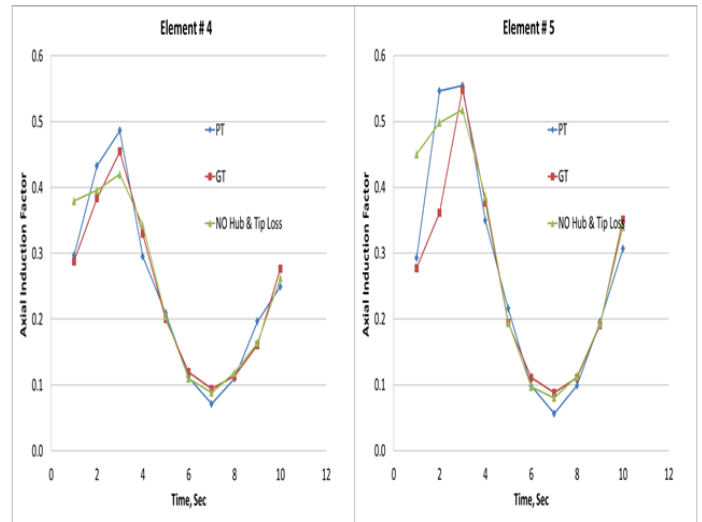


Fig. 27. Comparison of tangential induction factor for the elements 14-17 over a complete pitching motion cycle at $U_{\infty} = 8\text{m/s}$

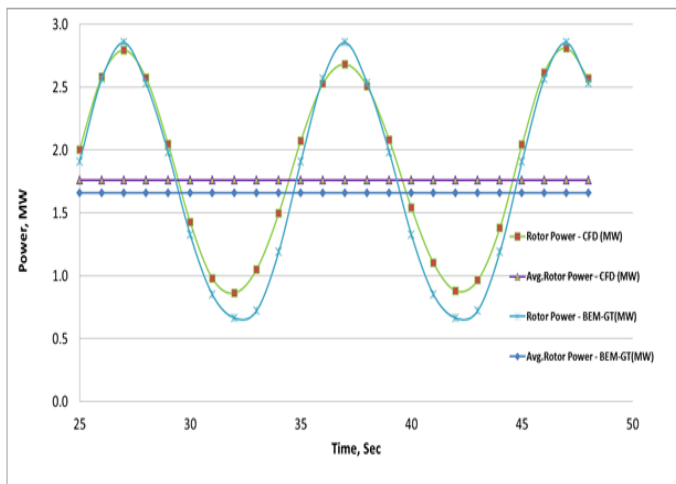


B. Comparison of Power Curves for a Pitching Rotor

FOWT are simultaneously subjected to aerodynamic, hydrodynamic and mooring line forces which are dynamic in nature inducing the platform motion in 6 degrees of freedom. These motions potentially amplify the unsteady aerodynamic effects (e.g. Blade-vortex interaction, Dynamic Stall, skewed inflow), which cannot be accurately simulated by current design methods based on the blade element momentum theory with common corrections as shown in Fig. 2-3. Blade – wake / vortex interaction effects are observed due to significant rotor plane displacement rate for the chosen operating conditions for the current turbine. BEM and CFD based rotor power predictions and its fluctuations are compared by choosing, 25-50 sec simulation results in one simulation cycle. As it is seen from Fig. 28, BEM predicted power is slightly lower (5.8%) compared to CFD based results, when the rotor pitches from the leeward direction to windward direction. When the rotor pitches against the wind, the difference between maximum peak power prediction by BEM and CFD is close to 0.1MW, whereas 0.2MW difference is minimum power prediction when the rotor pitching align with the wind direction due to strong interaction between blade and its own wake. BEM (AeroDyn) based rotor power/load fluctuation is high, which will have a direct impact on the blade design, as it will affect the fatigue loading. The average rotor power is 1.761 MW and 1.659 MW for CFD and BEM respectively.

VII. CONCLUSION

A high fidelity CFD based study has been carried out for floating offshore wind turbines (5MW NREL turbine) with the intention of validating the standard BEM theory. A minimum wave height of 12 m will push the turbine to operate in the turbulent state, which facilitate the comparison of BEM and CFD based induction factor derivation, as the aerodynamic force calculation rely on how accurate these factors are computed. A dynamic mesh methodology has been developed for accurate modelling of the platform pitching motion and its dynamic effects on the rotor. It is found from the results that 12-m wave height simulation leads to the turbine operating in the turbulent wake state as per BEM predictions. At this specific load case, the trend of elemental power values obtained from BEM equations agree well with the CFD results in most part of the blade except near the tip. The power prediction is high near the tip and it is attributed to the tip loss models used in BEM. There are notable differences in the elemental thrust values between BEM and CFD predictions. The current study concludes that the chosen CFD methodologies played their part well in capturing aerodynamic effects of pitching motion. From the results, it is clear that the dynamic power fluctuations are higher in BEM.



VIII. FUTURE WORK

As discussed in the previous sections the BEM based methods employs an iterative approach to calculate the aerodynamic forces derived from the induction factors obtained through empirical formulae which contain Glauert correction and tip and hub loss factors. To obtain the CFD based induction factor, BEM thrust equation including corrective terms has to be equated with CFD thrust force to derive the axial induction factor. This calls for another iterative process and to be validated for the new tip loss model which can predict very close to actual or CFD results. Comparison between BEM and CFD axial induction factors and model validation are to be performed. Moreover, all possible operating conditions will be considered and an attempt will be made to formulate suitable

Fig. 28. Total power at the rotor. Comparison against the relative wind speed experienced by the rotor due to platform pitching motion

correction terms with thrust equation of BEM to arrive at the CFD based induction factors derivation for the turbine working under turbulent wake state and vortex ring state.

REFERENCES

- [1]. UK government renewable energy targets, <https://www.gov.uk/government/policies/increasing-the-use-of-low-carbon-technologies>, accessed 27th November 2013
- [2]. EU renewable energy targets, http://ec.europa.eu/energy/renewables/targets_en.htm, accessed 27th November 2013
- [3]. Updated Capital Cost Estimates for Utility Scale Electricity Generating Plants (2013), U.S. Energy http://www.eia.gov/forecasts/capitalcost/pdf/updated_capcost.pdf, accessed 27th November 2013
- [4]. Musial, W et al (2004), "Feasibility of Floating Platform Systems for Wind Turbines", 23rd ASME Wind Energy Symposium
- [5]. Statoil website, Hywind information, <http://www.statoil.com/en/technologyinnovation/newenergy/renewablepowerproduction/offshore/hywind/pages/hywindputtingwindpowertothetest.aspx>, accessed 27th November 2013
- [6]. Windfloat press release, http://www.principlepowerinc.com/news/press_PPI_WF_deployment.html, accessed 27th November 2013
- [7]. Burton, T. et al, Wind Energy Handbook, ISBN 13: 978-0-471-48997-9
- [8]. Matha, D et al (2011), "Challenges in Simulation of Aerodynamics, Hydrodynamics, and Mooring-Line Dynamics of Floating Offshore Wind Turbines" - International Offshore and Polar Engineering Conference 2011
- [9]. Krishnamoorthi Sivalingam et al (2015), "Effects Of Platform Pitching Motion On Floating Offshore Wind Turbine (FOWT) Rotor", Offshore Technology Conference, Houston, Texas, USA
- [10]. Anand Bahuguni et al (2014), "Implementation of Computational Methods to Obtain Accurate Induction Factors for Offshore Wind Turbines" Volume 9B: Ocean Renewable Energy, ASME 2014 33rd International Conference on Ocean, Offshore and Arctic Engineering
- [11]. Jonkman, J. et al (2010). "Offshore Code Comparison Collaboration within IEA Wind Task 23: Phase IV Results Regarding Floating Wind Turbine Modeling". EWEC, NREL/CP-500-47534, 1-23
- [12]. Thomas Sebastian et al (2011), "Offshore Floating Wind Turbines - An Aerodynamic Perspective", 49th AIAA Aerospace Sciences Meeting including the New Horizons Forum and Aerospace Exposition, 4 - 7 January 2011, Orlando, Florida
- [13]. Peters, D. and Chen, S., "Momentum Theory, Dynamic Inflow, and the Vortex-Ring State," Journal of the American Helicopter Society, Vol. 27, No. 3, 1982, pp. 18-24
- [14]. Suzuki, A., Application of Dynamic Inflow Theory to Wind Turbine Rotors, Doctoral dissertation, University of Utah
- [15]. Jonkman, J. et al (2004). FAST User's Guide, NREL/EL-500-29798, Golden, CO: National Renewable Energy Laboratory, USA
- [16]. P.J. Moriarty et al (2005), AeroDyn Theory Manual, Technical Report, NREL/TP-500-36881, National Renewable Energy Laboratory, USA
- [17]. Jonkman, J. et al (2007). "Definition of a 5-MW Reference Wind Turbine for Offshore System Development", NREL/TP-500-38060, Golden, CO: National Renewable Energy Laboratory, USA.
- [18]. Jonkman, J. et al (2010). "Offshore Code Comparison Collaboration (OC3) for IEA Task 23 Offshore Wind Technology and Deployment". Technical Report, NREL/TP-5000-48191
- [19]. Raymond Chow et al (2011). "Verification of computational simulations of the NREL 5 MW rotor with a focus on inboard flow separation", Wind Energy, Wind Energy. 2012; 15:967-981
- [20]. David A. Corson et al (2012). "Investigating Aeroelastic Performance of Multi-MegaWatt Wind Turbine Rotors Using CFD", 53rd AIAA/ASME/ASCE/AHS/ASC Structures, Structural Dynamics and Materials Conference, AIAA 2012-1827